MASTER COPY KEEP THIS COPY FOR REPRODUCTION PURPOSES

REPORT DOCUMENTATION

AD-A257 062

1. AGENCY USE ONLY (Leave blank)	2. REPORT DATE	3. REPORT TYPE AND DATES COVERED
	August 31, 1992	Final Technical Report 7/15/89 - 10-14-91

4. TITLE AND SUBTITLE
Development of a 500-GHz Optoelectronic Modulator Using Superconducting Transmission Lines

5. FUNDING NUMBERS
DAAL03-89-K-0071

6. AUTHOR(S)
Steven L. Williamson
John A. Nees
Gerard Mourou, Principal Investigator

7. PERFORMING ORGANIZATION NAME(S) AND ADDRESS(ES)
University of Michigan
Ultrafast Science Lab
2200 Bonisteel Blvd.
Ann Arbor, MI 48109-2099

8. PERFORMING ORGANIZATION REPORT NUMBER
026506-920-831

9. SPONSORING/MONITORING AGENCY NAME(S) AND ADDRESS(ES)
U. S. Army Research Office
P. O. Box 12211
Research Triangle Park, NC 27709-2211

10. SPONSORING/MONITORING AGENCY REPORT NUMBER
ARO 26760.3-EL

11. SUPPLEMENTARY NOTES
The view, opinions and/or findings contained in this report are those of the author(s) and should not be construed as an official Department of the Army position, policy, or decision, unless so designated by other documentation.

12a. DISTRIBUTION/AVAILABILITY STATEMENT
Approved for public release; distribution unlimited.

12b. DISTRIBUTION CODE

13. ABSTRACT *(Maximum 200 words)*
This contract was set in place to investigate the technologies necessary to demonstrate multi-hundred-GHz modulation of optical signals. Techniques for eliminating velocity mismatch and modal dispersion, the two major limitations on state-of-the-art modulators, are presented. Further work to reduce signal distortion due to skin effect losses in normal conductors is detailed. Associated problems of interconnects and test instrumentation are also treated.

14. SUBJECT TERMS	15. NUMBER OF PAGES
modulator, detector, high-powered picosecond switching, Semiconductor Optical Temporal Analyzer (SOTA), picosecond nanoprobe	27
	16. PRICE CODE

17. SECURITY CLASSIFICATION OF REPORT	18. SECURITY CLASSIFICATION OF THIS PAGE	19. SECURITY CLASSIFICATION OF ABSTRACT	20. LIMITATION OF ABSTRACT
UNCLASSIFIED	UNCLASSIFIED	UNCLASSIFIED	UL

Final Report ARO

REPORT #026506-920-831

CONTRACT #DAAL03-89-K-0071

DEVELOPMENT OF A 500-GHz OPTOELECTRONIC MODULATOR USING SUPERCONDUCTING TRANSMISSION LINES

Steven L. Williamson, John A. Nees
Gerard Mourou, Principal Investigator
University of Michigan
Ultrafast Science Laboratory
2200 Bonisteel Blvd.
Ann Arbor, MI 48109-2099

August 31, 1992

Final Technical Report

Prepared for:

U.S. Army Research Office
PO Box 12211
Research Triangle Park, NC 27709-2211

Patsy S. Ashe
Contracting Officer

Robert Trew
Scientific Program Officer

DEVELOPMENT OF A 500-GHz OPTOELECTRONIC MODULATOR USING SUPERCONDUCTING TRANSMISSION LINES

GERARD A. MOUROU, PI

Abstract

This contract was set in place to investigate the technologies necessary to demonstrate multi-hundred-GHz modulation of optical signals. Techniques for eliminating velocity mismatch and modal dispersion, the two major limitations on state-of-the-art modulators, are presented. Further work to reduce signal distortion due to skin effect losses in normal conductors is detailed. Associated problems of interconnects and test instrumentation are also treated.

Table of Contents

Introduction

Optical fiber communication holds the potential for transmission rates beyond 1 terabit/s. The state-of-the-art in system bandwidth, however, lags behind by two orders of magnitude. This is due, in part, to our inability to measure the picosecond electrical transients that are present in the optoelectronic components. The development of electro-optic sampling enables time resolution of electrical transients with subpicosecond precision.[1] With this capability in hand, the development of modulators and detectors designed for bandwidths up to hundreds of GHz has become manageable. In the sections that follow we describe the development of a wavelength-compatible **modulator**, and **detector** for operation in the multi-hundred-GHz regime, as well as **high-power picosecond switching** and the newly developed **Semiconductor Optical Temporal Analyzer** (SOTA) and **picosecond nanoprobe**.

Modulator

Although optical fibers are capable of tremendous information capacity current sytems do not ultilze a major portion of the available bandwidth. Modulators designed for low voltage applications are currently limited to ~40 GHz.[2] In principle, a traveling-wave electro-optic modulator can be fabricated fabricated from GaAs, for modulation above 500 GHz. To approach such performance requires the elimination of not only velocity mismatch, which limits state-of-the-art devices. but also, dispersion of the microwave signal, radiation loss, and losses due to skin effect and free carrier absorption (figure **1**).

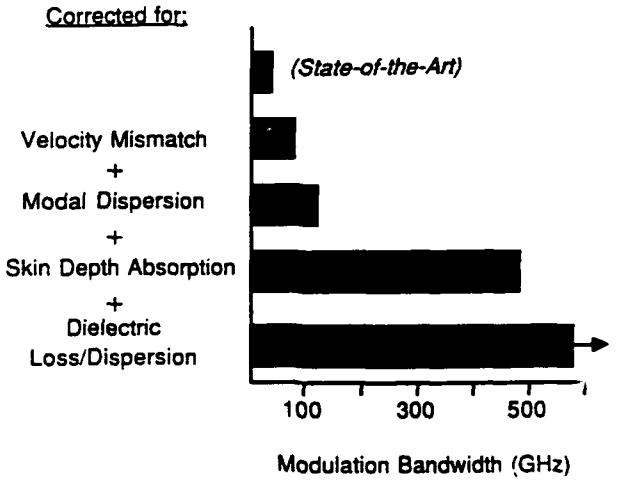

Figure 1 Fundamental limits for traveling-wave modulators

The primary source of dispersion, namely, velocity mismatch, is eliminated by encapsulating the transmission lines in a uniform GaAs medium. GaAs possesses the unique property of having bulk dielectric constants in the near infrared and millimeter-wave regimes that are essentially equal.[3] We have shown that encapsulating a transmission line in a uniform dielectric also eliminates frequency-dependent dispersion and

radiation losses otherwise present due to dielectric mismatch. Furthermore, losses associated with skin effect, and free-carrier absorption have been mitigated by lowering temperature.

We have shown dramatic enhancement in bandwidth by applying an index-matched superstrate using a straight, optically guided traveling-wave modulator.[4] In figure **2** a cross-sectional diagram of a GaAs traveling-wave modulator is depicted, with a GaAs superstrate positioned over the transmission line electrodes. The modulator is 4 mm in length. To test the bandwidth of the modulator a 1-ps risetime electrical pulse is generated using the technique of photoconductive sliding-contact switching.[5] A 1-ps optical probe pulse at 1064 nm is synchronized to the electrical pulse using an adjustable delay and is focused into the optical waveguide. Figure **3** shows the correlation of the electrical and optical signals over the 4 mm interaction length as the optical pulse is delayed relative to the electrical pulse timing. The 3.2 ps risetime corresponds to a bandwidth of 110 GHz.

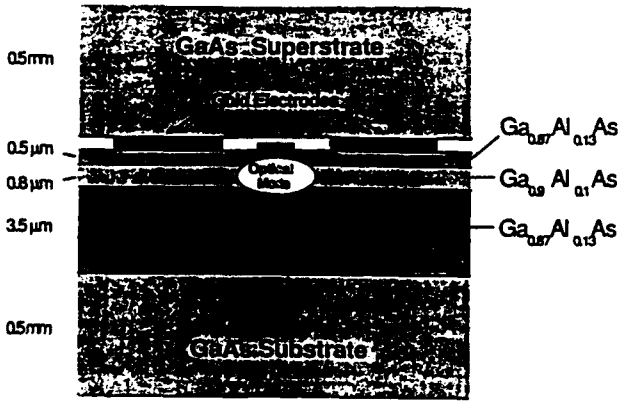

Figure 2 Crossection of a 110 GHz traveling-wave modulator

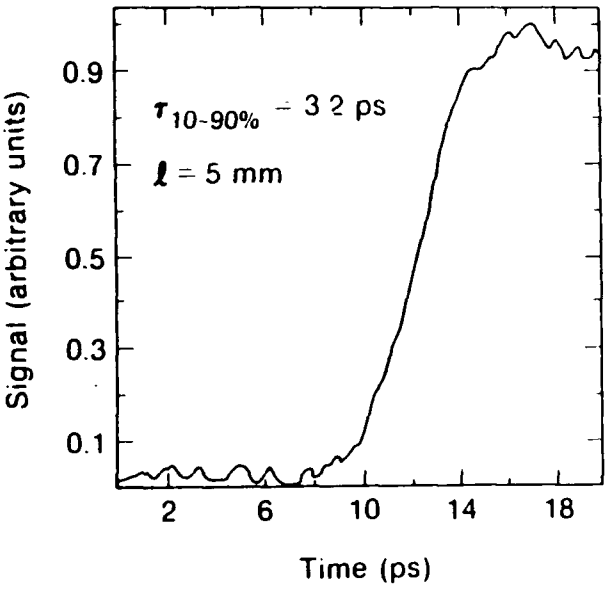

Figure 3 Correlation of a 1-ps optical pulse with a 1-ps electrical pulse on the modulator

This is the fastest traveling-wave modulator demonstrated to date. However, many problems beset this initial device. The optical waveguide is lossy for the 1064 nm, resulting in a 20-dB optical insertion loss. Also, the half-wave voltage is 288 volts, four times greater than the calculated value. These two effects are coupled and are a consequence of carrier generation from the optical probe pulse. Operation at cryogenic temperatures acts to steepen the absorption edge for the AlGaAs, thereby lowering the attenuation factor and enhancing the electric field . Operation at 1300 nm or longer wavelength also markedly decreases free carrier absorption.

To futher test the propagation of electrical signals on the modulator we have constructed a coplanar transmission line fully encapsulated in unintetionally doped [001] GaAs. By first reactive-ion etching 280 nm-deep coplanar troughs into which 280nm of gold is deposited, A pair of electrodes which are 20 μm wide and separated by 20 μm are formed leaving the top surface of the modulator flush. A scanning electron view of this stucture can be seen in figures **4**. The *dc* resistance/millimeter is 4.9 Ω/mm at 293 K and 0.8 Ω/mm at 10 K. A second wafer of GaAs is then placed on top fully enclosing the coplanar electrodes with, at most, 20 nm of air interface. The two wafers are kept together using spring-loaded clips to assure good contact. The presence of any gap at the interface will alter the effective dielectric constant for the electrical signal. An air gap of only 200 nm is sufficient to alter the propagation time by 2 ps.

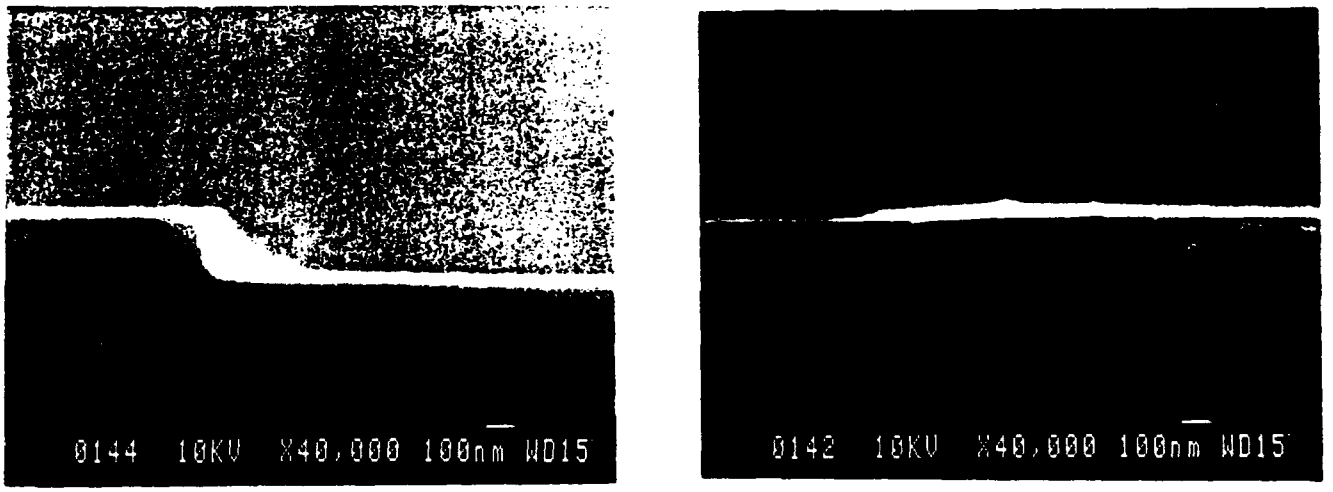

Figure 4a Scanning electron view of 280-nm channels **b Scanning electron view of flush coplanar striplines**

External electro-optic sampling was used to characterize the device. A picosecond electrical pulse propagated round-trip on the transmission lines, accumulating 10 mm of travel, before being measured (see figure **5**). Figures **6** and **7** show the resultant signals at 293 K and 10 K respectively. The input risetime at both temperatures is a 1.3 ps pulse. The output at 293 K is found to have been strongly attenuated and the risetime broadened to 3.0 ps for a response of 2.1 ps after deconvoluting the input. Both effects are primarily due to skin effect attenuation by the gold electrodes. At 10 K the amplitude of the propagated signal is comparable to the input and the risetime is 2.0 ps, corresponding to a response of 1.4 ps, for a bandwidth of 250 GHz. This broadening takes place over a total propagation time of 120 ps.

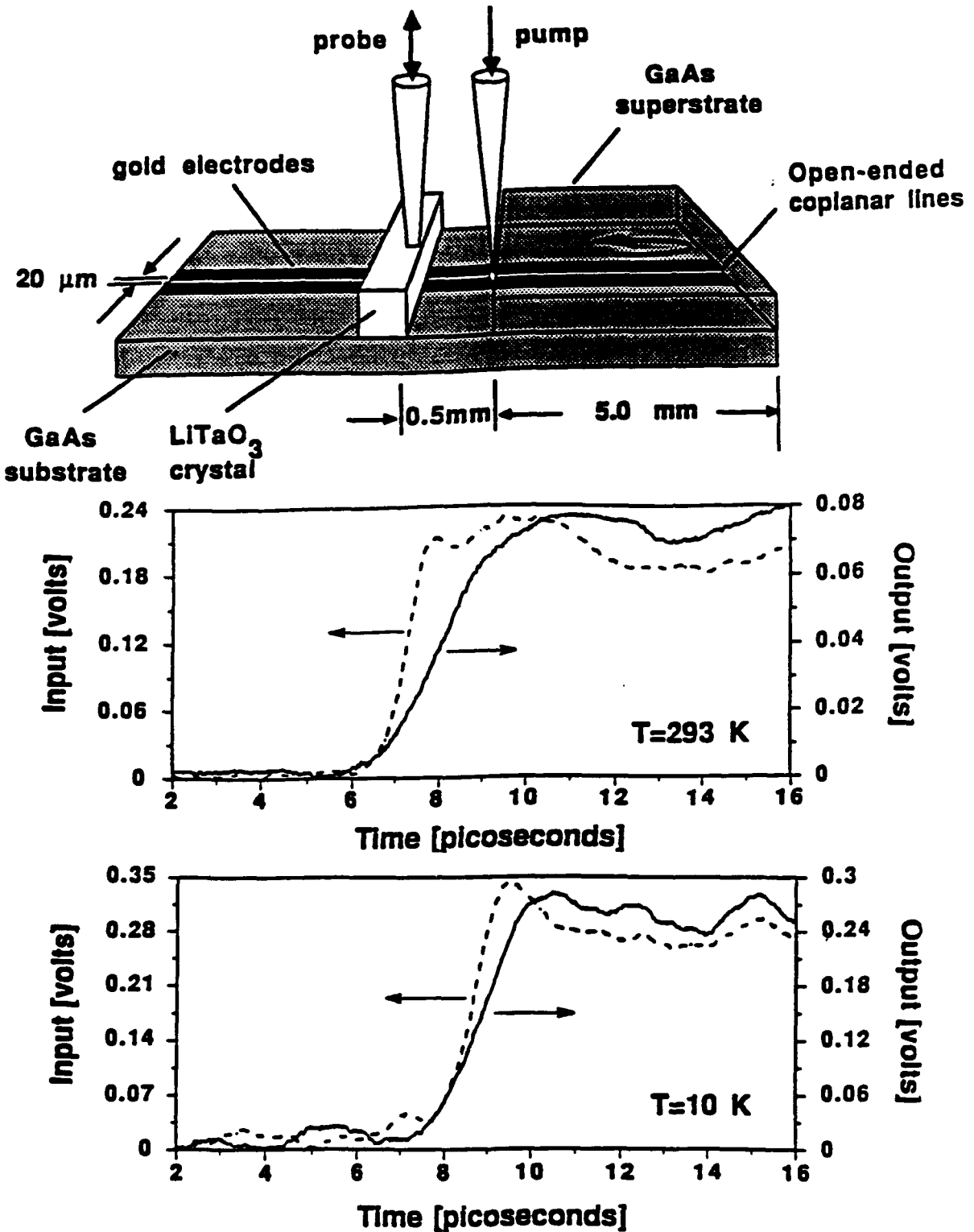

Figures 5, 6, and 7 5) Illustration of the experimental measurement of electrical propagation delay, 6) Input and output after 10mm propagation at room teperature, 7) Input and output after 10mm propagation at 10 K

A careful determination of the propagation time was made by measuring the optical path difference between optical pulses synchronized with the arrival of the input and output signals. By knowing the propagation time and the length of the superstrate an accurate measurement of the effective dielectric constant can be determined. The effective dielectric constant was found to be 11.60 (+/- 0.02). This value agrees remarkably well with the bulk value of GaAs at 1.3 μm, 11.62 [3]. The difference in arrival times between electrical and optical pulses propagating in this structure would amount to ~500 fs for a 10 mm interaction length.

The results are qualitatively revealing. The use of a mechanically-applied GaAs superstrate has served to demonstrate the feasibility of velocity matching for ultrafast travelling-wave optoelectronic modulators. Practical use of this technique is being realized by regrowing GaAs over the substrate forming a superstrate that is an integral part of the device. Regrowth techniques are now being investigated for compatibility with various electrode structures and compositions.

Detector

Also of key importance in the development of multi-hundred-GHz optical communications, is the detector. Much progress has been made over the past several years in the development of high-speed photodiode detectors. A detection bandwidth of 105 GHz together with a responsivity of 0.1 A/W have been reported for a metal-semiconductor-metal (MSM) photodiode.[6] The most common approach to increasing the bandwidth in MSM photodiodes (at least up to 100 GHz) is to shorten the carrier transit time by reducing the electrode spacing. However, achievement of bandwidths > 100 GHz requires more than simply reducing further the electrode spacing. Monte Carlo simulation of the intrinsic response for a photodiode with 0.1-μm electrode spacing shows a response tail persisting for picoseconds and having an integrated energy comparable to the main signal.[7,8] This tail is caused by the long transit time of the

photogenerated holes, which is almost 10 times that of electrons. This can be seen experimentally in figure **8** which shows the response of a 0.6 μm spacing interdigital MSM photodiode on semi-insulating GaAs. As illustrated in figure **9**, the persistence of conductivity is attributed to the low mobility of the holes which results in low charge collection and recombination rates.

Response times of photoconductive detectors, on the other hand, can be quite fast because they are determined solely by the carrier lifetime of the material that is used. Recently, low-temperature-grown GaAs (LT-GaAs) has been applied to ultrafast [9] and high-power [10] optical switching. The subpicosecond carrier lifetime,[11] high mobility (> 200 $cm^2/V \cdot s$), and high breakdown field strength (>100 kV/cm) of LT GaAs make this material ideal for electrical pulse generation and gating. Such applications have so far required the use of moderate-to-high peak optical powers since the switching efficiency, defined as the ratio of electrical output power to optical input power, is still < 1%. However, as we have found, the *switching efficiency* tends to be influenced more by the electrode dimensions than by the intrinsic characteristics of the material.

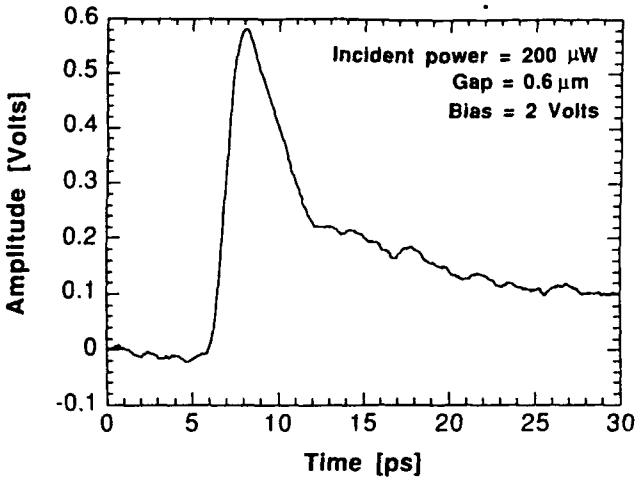

Figure 8 Response of a 0.6μm interdigital MSM on GaAs

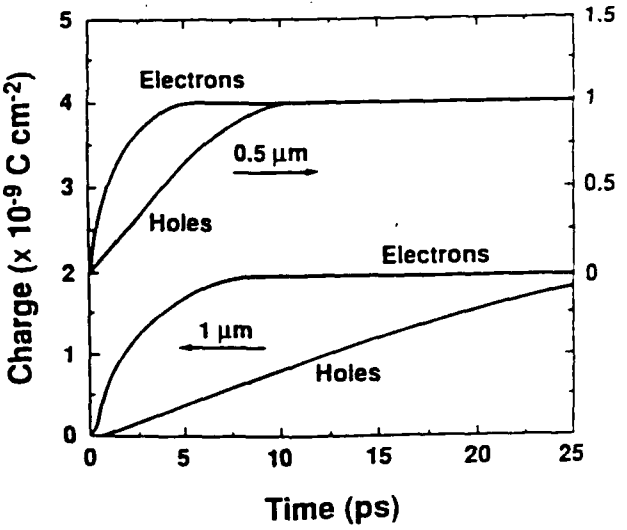

Figure 9 Electron and hole collection rates for 0.5- and 1-μm interdigital MSMs

We report on an LT-GaAs-based photoconductive detector that takes advantage of the high breakdown field capability of LT-GaAs to greatly improve sensitivity. In a photodiode, a reduction in electrode spacing improves speed with little change in sensitivity. In a photoconductive detector, by contrast, such a reduction increases the sensitivity with little change in speed. Decreasing the carrier transit time across the semiconductor gap to a value comparable to the carrier lifetime increases the photocurrent gain to a value of unity.[12] For a carrier lifetime of 1 ps, this condition is met when the electrode spacing, i.e., the actual gap between electrodes, is 0.1 μm. A further decrease in the electrode spacing could increase the photoconductive gain to an even higher value, provided the metal-semiconductor contacts are ohmic. With unity gain, the responsivity of a LT GaAs photoconductive detector becomes comparable to that of a photodiode, while its speed is still dominated by the (sub)picosecond intrinsic carrier lifetime.

To demonstrate this principle, we fabricated an LT-GaAs photoconductive detector with interdigitatal electrodes having finger widths and spacings of 0.2 μm, as shown in figure **10**. A 1.5-μm-thick LT-GaAs layer was grown on a (100) semi-insulating GaAs substrate having a 0.4-μm-thick conventionally grown undoped buffer layer. The LT-GaAs layer growth was performed using molecular beam epitaxy with a substrate temperature of 190 °C, followed by annealing at 600 °C for 10 min in an arsenic overpressure. The interdigitatal electrodes were fabricated of 300-Å/2000-Å Ti/Au using a JEOL JBX 5DIIF direct-write electron-beam lithography system. The active area of the detector is 6.5 x 7.6 μm^2. Coplanar transmission line electrodes of 500-Å/2500-Å Ti/Au, with 20-μm widths and spacings and 5-mm lengths, were also fabricated on the LT GaAs using conventional optical lithography. For comparative purposes, similar structures were also fabricated with 0.6- and1.0-μm finger spacings and widths.

Figure 10 Scanning electron view of a 0.2 μm interdigital MSM on LT-GaAs

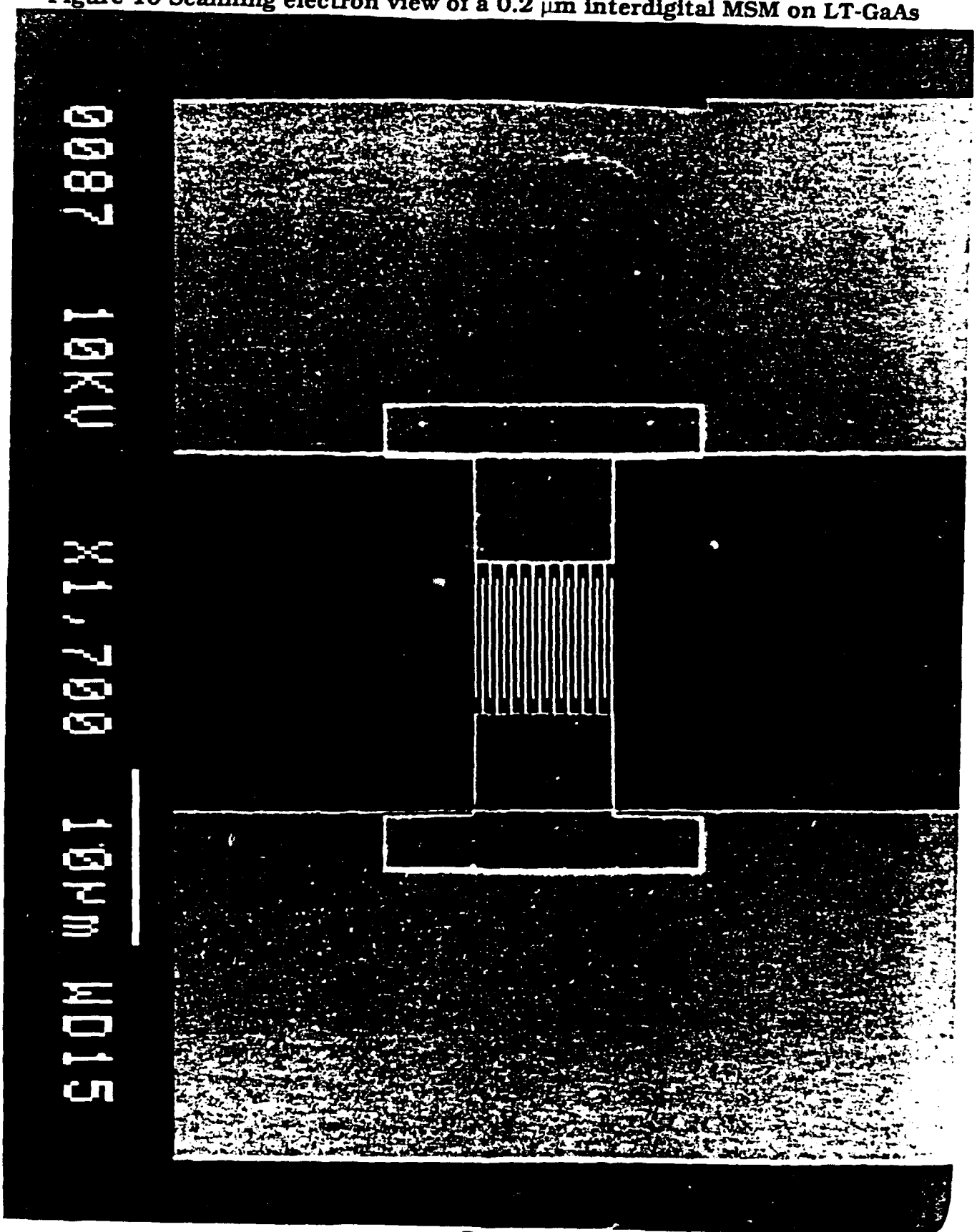

Referring to figure **10**, the LT-GaAs photoconductive detector was placed between coplanar transmission lines (Z_0 = 90 Ω) to assure good coupling of the generated electrical pulse to the propagating mode and also to eliminate parasitic losses. The detector was not antireflection (AR) coated in this initial work. A reference transmission line of identical dimensions, but without the interdigitatal detector, was also fabricated on the wafer to determine the system response. The technique of sliding-contact switching, which provides electrical excitation between the lines without the interdigitatal detector, can have a response < 0.5 ps.[5] The photoconductive detectors were characterized using the technique of external electrooptic (EO) sampling [1]. A balanced, colliding-pulse, mode-locked dye laser operating at 610 nm with a repetition rate of 100 MHz was used, to produce150-fs pump and probe pulses. Electrical signals were measured on the transmission line at a distance of 450 μm from the detector. Although not shown in the figure, the EO sampling crystal spanned both the detector/transmission-line assembly and the reference transmission line, so that the translation of the pump and probe beams required to make either measurement was only ~ 200 μm.

A bias of 10 V dc was applied to the detector before breakdown occurred, corresponding to a breakdown field strength of 500 kV/cm. This value is more than twice the highest that has been reported for LT GaAs under dc-bias conditions, which was obtained using 20-μm-spaced electrodes.[9] Our result represents the better measurement of the actual breakdown field strength for LT-GaAs, since our 0.2-μm electrode spacing confines the electric field to the 1.5-μm-thick LT GaAs epilayer. The dark current for 1 V applied to the detector is 100 pA. At 8 V (400 kV/cm), where we chose to operate, the dark current increased to 300 nA. For an average optical power of 4 μW, the responsivity is 0.1 A/W. Past work using 20-μm-spaced electrodes on LT-GaAs attained a responsivity of only 10^{-3} A/W.[13] The 100-fold reduction in gap dimension therefore improves the responsivity 100 fold. The value of 0.1 A/W is comparable to that for the responsivity of high-speed photodiodes. The reflective losses at the surface from the interdigitated electrodes and the semiconductor amounted to 70% of the incident signal, for an internal quantum efficiency of 68%.

The intrinsic material response time for the LT GaAs sample was measured previously using an all-optical pump-probe technique [14] and found to be 0.6 ps. We calculate the capacitance [15] of our structure to be 4 fF, for an RC-limited response time of 360 fs. Figure **11** shows the measured responses for the detector/transmission-line assembly and the sliding-contact switch on the reference transmission line. Both measurements were obtained 450 μm from the point of signal generation. The optical pulse energy on the detector is 0.04 pJ (4-μW average power).

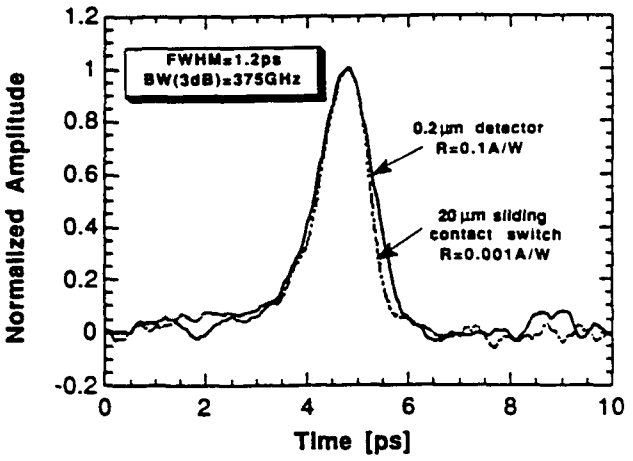

Figure 11 Temporal response of the photoconductive detector and sliding-contact switch measured 450 μm from the point of signal generation.

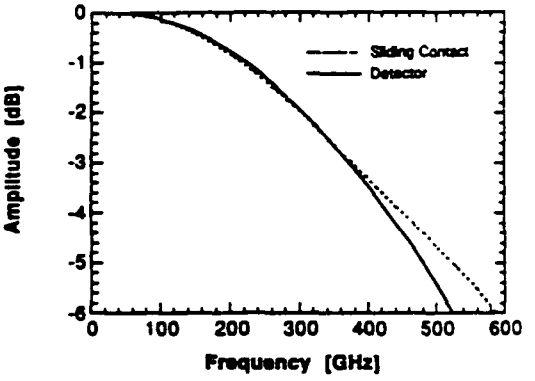

Figure 12 The -3-dB point for both signals occurs at 375 GHz.

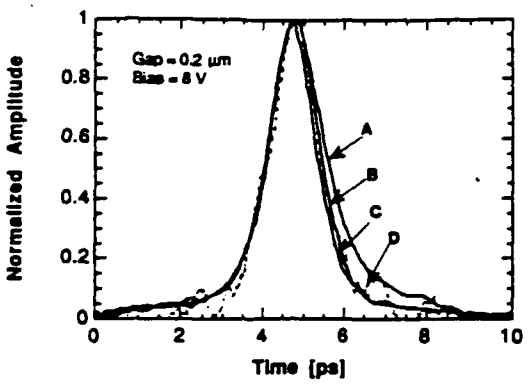

Figure 13 Set of four signals generated from the photoconductive detector,using 22 (A), 8.3 (B), 0.83 (C), and 0.04 (D) pJ, respectively.

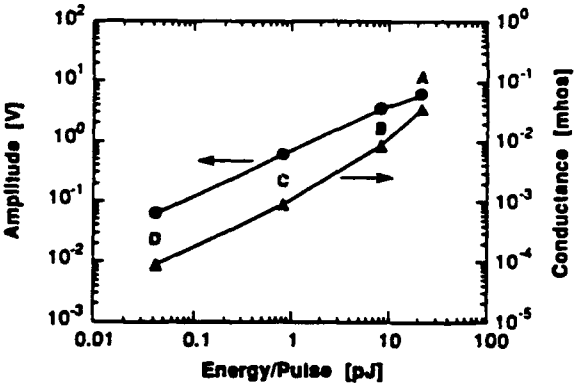

Figure 14 Peak amplitude vs. pulse energy for a 0.2-μm interdigital MSM on LT-GaAs

The full-width-at-half-maximum of the detector response is 1.2 ps with no evidence of a tail. In fact, the trailing edge, with a 10-90% fall time of 0.8 ps, is faster than the leading edge. We note a similar shape of the response for the sliding-contact switch on the reference transmission line. This is indicative of modal dispersion from quasi-TEM propagation along a transmission line having a substrate and superstrate with different permittivities.[16] Since the measured results are a convolution of the LT-GaAs intrinsic response time and such system-related factors as the RC time constant, laser pulse width, and electrooptic material response, the intrinsic response time for the interdigitatal detector may be subpicosecond. The -3-dB point, shown in figure **12**, for both signals occurs

at 375 GHz, measured by taking their discrete Fourier transforms. A set of waveforms for several values of pulse energy is shown in figure **13**. The four signals have peak amplitudes of 0.06 , 0.6 , 3.5 , and 6 V generated using 0.04, 0.83, 8.3, and 22 pJ/pulse respectively. Figure **14** shows the peak amplitude and conductivity of these signals plotted against optical pulse energy. We see that a nearly 500-fold increase in intensity expands the response only slightly from 1.2 to 1.5 ps. Under similar experimental conditions, a high-speed photodiode would suffer significant temporal broadening from space charge [17] and from low-frequency gain by photoinduced band bending.[18] Thus, the LT-GaAs photoconductive detector avoids the usual restriction of photodiodes to pulse energies below 0.1 pJ.

In figure **15** we show the electric-field dependence for the 0.2 μm detector. Measurements were made with electric field strengths of 25 V/μm, 15 V/μm, and 5 V/μm. There is little change in the pulse width, and in particular, the decay time with electric field. A similar measurement was carried out for the 1.0 μm detector, as shown in figure **16**. Here, there is a noticeable increase in decay time with an electric field as low as 10 V/μm. One possible explanation for the gap dependance on decay time involves the process of impact ionization.[19] When the electric field exceeds a certain value, photoinduced carriers can accelerate to an energy large enough to ionize additional carriers. The occurrence of impact ionization will increase the decay time. The rate of ionization is dependent on both the electric field and electrode spacing. The field in both structures is well above the threshold value for impact ionization. However, the much shorter electrode spacing, in the case of the 0.2 μm structure, prevents the process from fully developing.

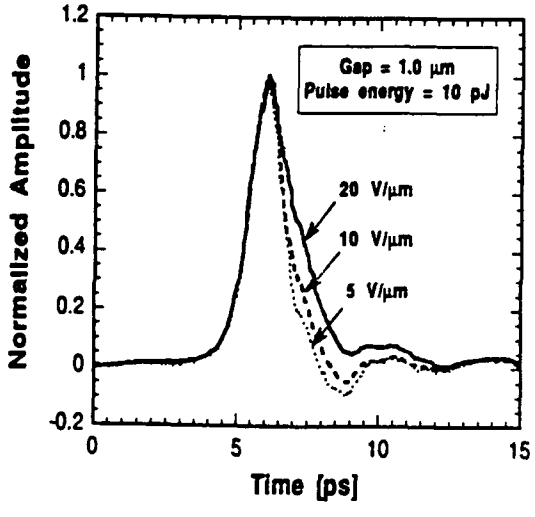

Figure 15 LT-GaAs photoconductive response as a function of electric field with electrode width and spacing of 0.2 μm,

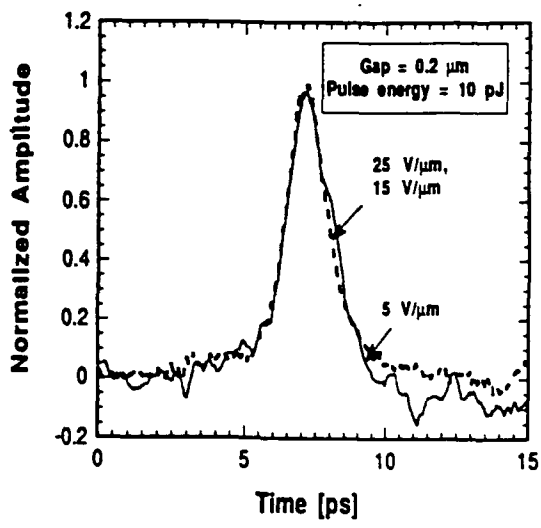

Figure 16 -with electrode width and spacing of 1.0 μm.

In short, we have developed a new MSM-type photoconductive detector, based on low-temperature-grown GaAs, fabricated using 0.2-μm-spaced interdigitatal electrodes. The response time measured directly by EO sampling, *i.e.*, without deconvolution, is 1.2 ps. With no AR coating on the detector, the responsivity is 0.1 A/W. To our knowledge, this is the fastest high-sensitivity photoconductive detector of any kind reported to date. In addition, it can be driven to an on-state resistance of 30 Ω with little degradation in speed. This versatility permits the device to function both as a detector and a switch. In the switching mode, the device can perform either as a high-contrast gate with a picosecond window or as an efficient picosecond electrical-pulse generator. Such unique dual functionality together with ease of integration will permit a number of detector elements to be combined for acquiring and processing single-picosecond optical and electrical events with high efficiency and minimal temporal distortion.

High-Power Switching

The unique properties of the LT-GaAs material which make it so attractive for high-speed MSM photoconductors also give the material a distinct advantage in other applications which push the limits of speed, field breakdown potential and dark resistivity. In order to further explore the utility of these epi-layers we have conducted a study of photocunductive switching at the kilovolt level with peak currents aproaching 20 Amps.

In recent years many applications have emerged for high-voltage, high-speed switching. The best technique now available for achieving kilovolt electrical pulses with picosecond risetimes is laser-driven photoconductive switching. To date, generation of a 1 kV pulse with risetime and pulsewidth of 12 ps and 70 ps, respectively has been reported [20]. This was accomplished using a high-resistivity semiconductor with a 1.5 mm switch gap. The fastest risetime that is possible for this switching structure can be determined by calculating the propagation time over a distance equal to the switching gap. For this size gap a risetime of ~12 ps is found. Using electrodes separated by 10 μm, subpicosecond duration electrical pulses with amplitudes up to 6 volts have also been laser-generated [13]. The competing needs of having a large photoconductive gap to hold off high voltage and a small gap to maintain high speed have hitherto left kilovolt amplitude and single picosecond pulse generation decoupled.

With the advent of Low-Temperature Molecular-Beam-Epitaxy-grown GaAs (LT-GaAs) it is possible to fabricate extremely high resistivity, high breakdown threshold switches. Now, *dc* electric fields in excess of 10^5 V/cm are routinely achieved. It is also possible to take advantage of the finite time necessary for thermal runaway or impact ionization to evolve by pulse-biasing the switching element for times shorter than breakdown [1]. Using LT-GaAs and the technique of pulse biasing we have applied up to 1.3 kV to a 100 μm gap. With this gap dimension, switching of the kilovolt-bias requires less than 1 μJ of optical energy, obtainable with an amplified subpicosecond dye laser.

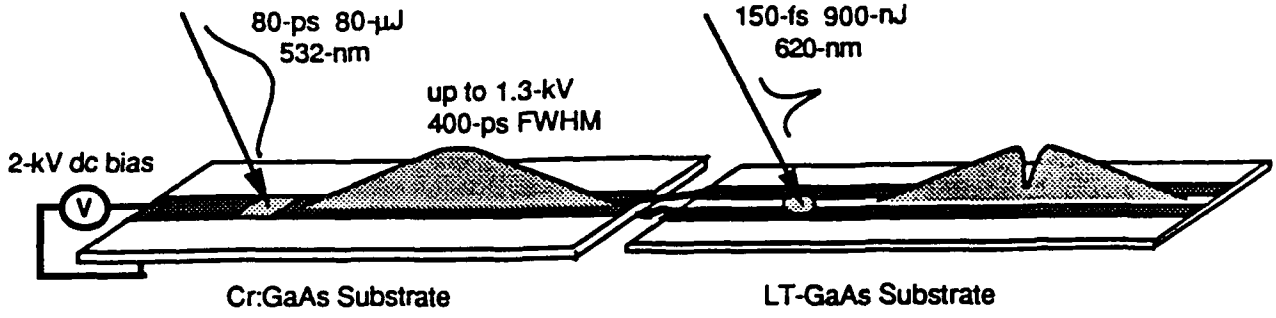

Figure 17 High power switching experimental set-up

A schematic diagram of the experimental configuration is shown in figure **17** Our laser generates 150 fs, 2 μJ pulses at 620 nm with a 2-kHz repetition rate, using a two-stage dye amplifier pumped by a frequency doubled Nd:YAG regenerative amplifier.[21, 22] Part of the frequency-doubled Nd:YAG regenerative amplifier output is used to excite a dc-biased 4-mm-long semi-insulating-GaAs switch which is used as the pulse-bias network. The switch is mounted in a microstrip line geometry between a ~10 Ω charge line and a 90 Ω transmission line. Illuminated by an 80 μJ, 80 ps optical pulse at 532 nm, this device produces an electrical pulse which has an amplitude equal to 70% of the dc bias voltage (up to 2 kV) and a duration of 400 ps. This pulse then biases a 90 Ω coplanar stripline (100 μm wide gold conductors separated by 100 μm) on a LT-GaAs substrate. As the bias pulse propagates along the transmission lines, a 150 fs, submicrojoule optical pulse excites the area between the lines. The high density of carriers formed within the LT-GaAs acts to short the electrodes. This form of sliding contact switching, in principle, allows total switching of the applied bias voltage [5]. External electro-optic sampling [1] in a $LiTaO_3$ crystal with a 150 fs pulse is used to measure the signal 300 μm from the switch site. In our configuration the crystal has a half-wave voltage of ~4 kV insuring a response linear within 2% over the range of voltages measured. The calibration error of the measurement is estimated to be +/- 5% owing mainly to laser intensity fluctuations. Waveforms are recorded for different settings of bias voltage and optical energy.

Figure **18** shows an 825-V pulse with risetime of 1.4 ps and a 4.0-ps duration (full-width-at-half-maximum). The negative precursor to the pulse is attributed to the radiation from the dipole formed at the generation site. For incident optical energies greater than 500 nJ we observe saturation of the voltage-switching efficiency, defined as the ratio of switched voltage to applied voltage, as shown in figure **19**. While the maximum efficiency is ideally 100%, the 70% experimentally measured can be explained by a combination of factors including dispersion and radiation of the propagating electrical pulse as well as contact resistance.

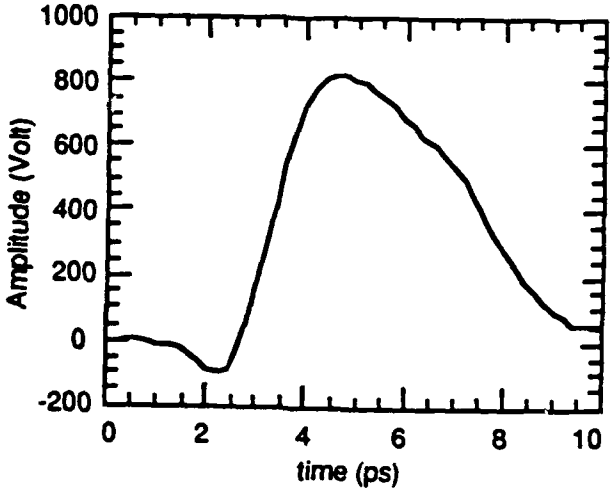

Figure 18 825 V pulse switched on 100-μm coplanar transmission lines on LT-GaAs

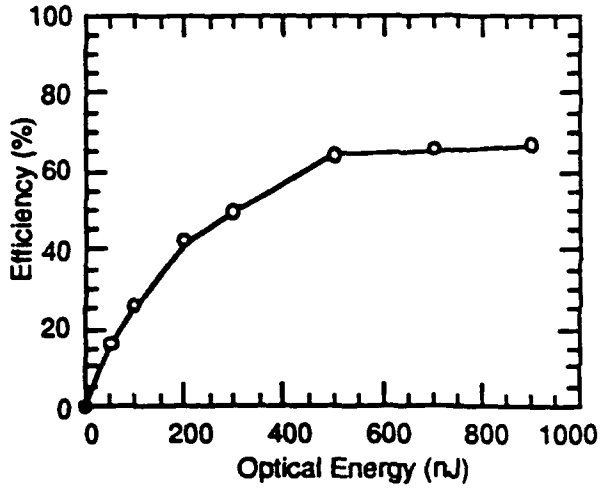

Figure 19 Switching efficiency (voltage switched/voltage biased) vs. optical energy

The rise time is ultimately limited by the 100-μm transmission line dimensions, however we also find a clear dependence on the carrier density. As illustrated in figure 4, we observe a degradation from 1.1 ps to 1.5 ps over the range of optical energy from 100 to 900 nJ. This corresponds to a saturation in the slew rate. The rise time nevertheless appears to be independent of the electric field (figure 5). The relation of the risetime to the carrier density is still not well understood. Explanations involving saturation of the current density and strong carrier scattering are presently being investigated.

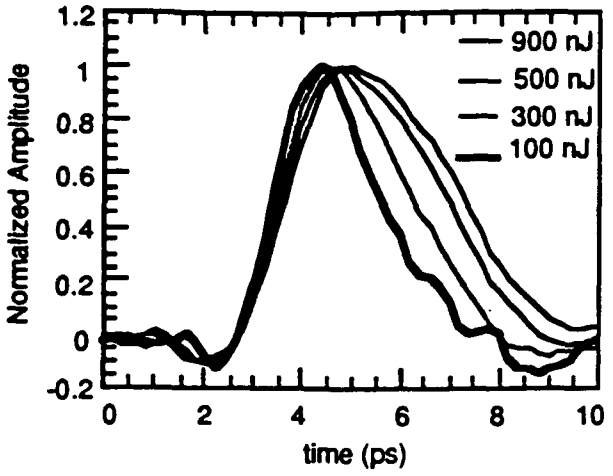

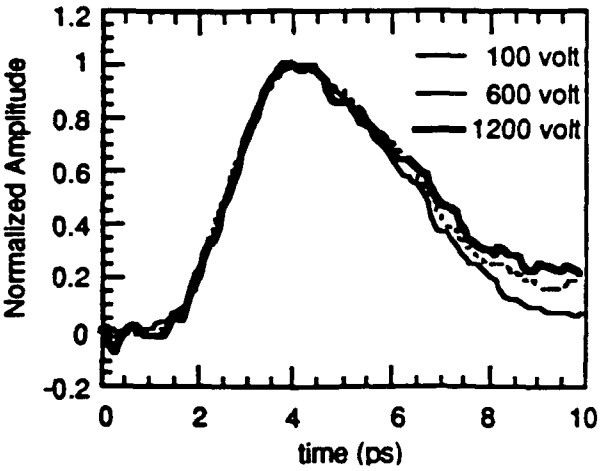

Figure20 Switch response for different optical pulse energies

Figure 21 Switch response for different applied voltages

Although a subpicosecond recombination-time was anticipated from previous work [13], our measurements reveal a much longer recovery time. The tail was also found to increase when either the carrier density or applied electric field were increased (figures **20** and **21**). Significant local heating due to the extremely high current densities (up to 10^7 A/cm^2) drawn through the switch area may result in generation of additional carriers and explain the long recovery time.

Another possible explanation for the long recombination time involves intervalley scattering which is known to be strongly dependent on both electric field and carrier density. The switched electric pulse shape reflects the evolution of the current density which is proportional to the product of carrier density and average carrier velocity. In GaAs, a photogenerated hot electron under the influence of a strong electric field can scatter from the central valley to the high-effective-mass satellite X- and L-valleys thereby reducing its velocity and ability to produce current.

The scattering probability increases with the electrical field and, under our experimental conditions, we estimate that more than 80% of the carriers scatter into the satellite valleys within 100 fs [23]. The transfer of those electrons back into the central valley can take several picoseconds [24]. As the pump energy increases so does the carrier density in the central valley. Consequently, the probability for an electron to scatter back into the central valley decreases. As the carriers in the central valley begin to recombine (within a few hundred femtoseconds for LT-GaAs), the probability of carrier transfer from the satellite valleys back to the central valley increases. The satellite valleys can then be seen as sources reinjecting hot electrons into the central valley at a rate dependent on the relative carrier populations which are function of optical fluence, electric field and wavelength. This process will cause current to persist until all carriers

transfer back to the central valley where they either are trapped or recombine.

In conclusion, we report on the application of LT-grown GaAs for photoconductive switching using a pulse bias technique leading to the generation of a 825 V pulse with 1.4 ps rise time and duration of 4.0 ps. This represents the highest voltage ever obtained on the single picosecond time scale. This new capability to produce ultrashort high peak power electrical pulses is of interest for applications in fields such as nonlinear millimeter-wave spectroscopy, radar, high-energy physics and ultrafast instrumentation.

Semiconductor Optical Temporal Analyzer

At far lower power levels high-speed, high-sensitivity photodetectors have been studied in other groups using the technique of picosecond photoconductive sampling.[25] Although the emphasis has been placed on the characterization of the detector,[26, 27] the combination of high-speed detector and sampling photogate can also be viewed as a high-speed optical correlator. To our knowledge, this configuration has not yet been applied to the measurement of optical waveforms. This is due, in part, to the relatively slow detectors that have been available. However, to have the highest speed and sensitivity requires more than simply a fast detector. Both the photodetector and photo-gate must have high speed *combined* with high sensitivity.

In this section we describe a novel 1.2 ps photoconductive detector that functions with high performance in either detection or gating mode and now permits monolithic integration of the two elements. This is the key ingredient in the development of a new optical temporal analyzer.

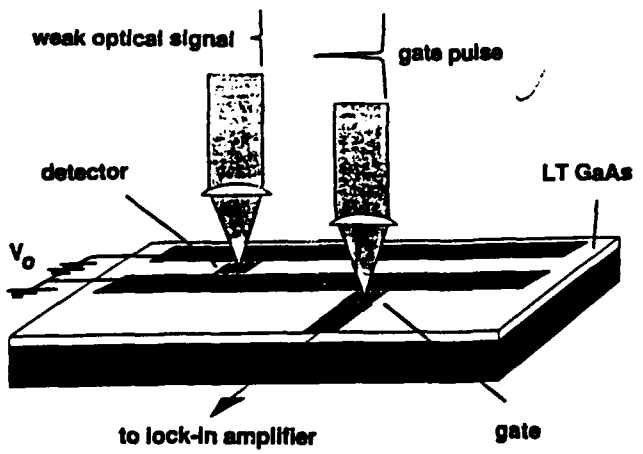

Figure 22 Experimental setup for testing the SOTA. The detector and gate are identical to one another and to the detector shown in figure 10.

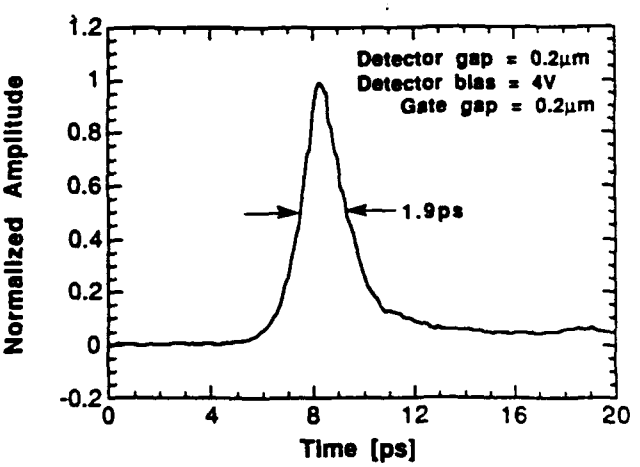

Figure 23 Temporal response from the SOTA.

Figure **22** depicts the experimental setup for the Semiconductor Optical Temporal Analyzer - SOTA. It is comprised of a fast detector and gate, integrated with a coplanar transmission line structure. The fast gate samples the electrical replica of the optical signal produced from the detector. The gate is located 100 μm from the detector. The gate electrode, fabricated perpendicular to the transmission line, is 1 mm in length. The detector and gate are identical to one another and to the detector described in the previous section. A CPM dye laser is again used as the pump/probe. The gate beam has an average power of 3 mW, while the pump beam is adjustable from 8 nW to 3 mW. The pump beam is chopped at the lock-in amplifier frequency of 500 Hz. The output from the gate detector is amplified using a current amplifier set at 10^{-7} volts/amp. The signal is further amplified using a lock-in amplifier.

Figure **23** shows a typical correlation curve measured with an average power on the detector of 1mW. The system response is 1.9 ps, matching the convolution value for the combined detector (1.2 ps) and gate (1.5 ps) responses. We notice that the correlation trace plateaus on its trailing edge. This tail was found to be independent of either the pump or gate pulse energies, indicating a possible rf-coupling effect to the gate electrode. The measured noise-equivalent-power (NEP), defined as the average optical power required to produce a signal-to-noise of one in a 1 Hz averaging bandwidth, is 500 pW.

The theoretical NEP for the SOTA is ultimately determined by the thermal, or *Johnson, noise at the photoconductive gate.*[28]

The thermal noise current is given by

$$i_{thermal} = \sqrt{4kTG}\ [A/\sqrt{Hz}]$$

where k is the Boltzman constant, T is the temperature, and G is the average conductance of the gate. The gate resistance is 10 MΩ in the off-state and 30 Ω in the on-state. With a duty cycle of 10^{-4} (1 ps gate window per 10 ns pulse period), this is equivalent to an average gate conductance of 3.4×10^{-6} mhos. At room temperature, the thermal noise current is 2.4×10^{-13} A/Hz$^{1/2}$. This corresponds to a theoretical NEP of 2 pW. The large discrepancy between the theoretical and measured NEP values is due to large RF pickup noise from the surrounding environment. Mitigation of this noise is presently underway.

It should be noted that this expression for thermal noise assumes a carrier collision time much faster than either the carrier lifetime or transit time.[29] With LT GaAs, the carrier collision time is comparable to carrier lifetime. A theoretical NEP of 2 pW may, in fact, be a conservative value.

We also see from this expression that the thermal noise current increases as the square root of the gate conductance. The signal current, on the other hand, increases linearly with gate conductance. The highest signal-to-noise is achieved when the gate is completely closed. An upper limit, however, exist for the gate conductance, imposed by the onset of carrier saturation. This effect, evident from the intensity-dependent

temporal broadening seen in figure 5, already degrades our system response by 10%.

In short, we have taken advantage of the features of the newly developed MSM photoconductive detector on LT-GaAs to develop a picosecond resolution, semiconductor optical temporal analyzer (SOTA). The measured NEP for the system is 500 pW. The technique is jitter-free, permitting long integration times. Ultraweak picosecond fluorescence and scattering experiments, as well as other ultrafast phenomena can be time-resolved using this relatively simple tool.

Picosecond Nanoprobe

The continuing advances made in the development of semiconductor devices have pushed the speed of some devices to frequencies in excess of 400 GHz [30]. To accurately test devices with this response requires the development of new probing techniques, capable of not only high temporal and spatial resolution, but also noninvasive inspection. Existing, purely electronic measurement instruments, such as vector network analyzers, spectrum analyzers, and sampling oscilloscopes, are not adequate tools for testing state-of-the-art high-speed integrated circuits. The rf network analyzer, which is now gaining acceptance for use up to 100 GHz, still has difficulties with test-fixture transitions, de-embedding of parasitic parameters, and overall accuracy and convenience of operation. Furthermore, internal nodes cannot be tested at high speeds with the low-impedance probe technology that is now available for use with such instruments.

In contrast to purely electrical approaches, electro-optic measurement techniques have many unique features for high-speed circuit testing. The major attribute gained from this marriage of optics and electronics is speed - both in temporal resolution, and in acquisition time. External-probe-electro-optic (EO) sampling has a temporal resolution as fast as 290-fs (>1 THz bandwidth) and offers the greatest flexibility of any optically-based technique now available.[1] External EO sampling uses a small (50-μm^2) tip of electric-field sensitive material ($LiTaO^3$ or $LiNbO^3$) to make measurements of fringing electric fields that extend above the circuit under test. In developing applications for this probe technology, extending from high-speed, non-loading pin testing of packaged devices, to development of a 100-GHz electro-optic network analyzer for testing of high-speed discrete analog devices[31], we also encountered limitations in spatial resolution (~5 μm) and signal sensitivity (>10 mV/√Hz). Also, absolute voltage measurements have been subject to interpretation.

We have recently developed a new optically-based external probe that promises to overcome these limitations while maintaining a temporal resolution of 1-ps. The probe concept is based on photoconductive (PC) sampling, which has the highest sensitivity of any optically-based sampling technique.[32] The probe we developed has a demonstrated sensitivity of 1 μV/√Hz and is capable of measuring the absolute voltage of the device-under-test. The dynamic range is $>10^6$, making possible measurements from the microvolt to the 10-volt level. The probe, though contacting in nature, is non-invasive with a load resistance of >100 kΩ and a capacitance of <0.1 fF. It makes contact to the device under test using a conical-shaped tip which

will have a tip radius of <100 nm. The sensitivity and speed of the probe are independent of the tip-to-device contact resistance up to 10 kΩ.

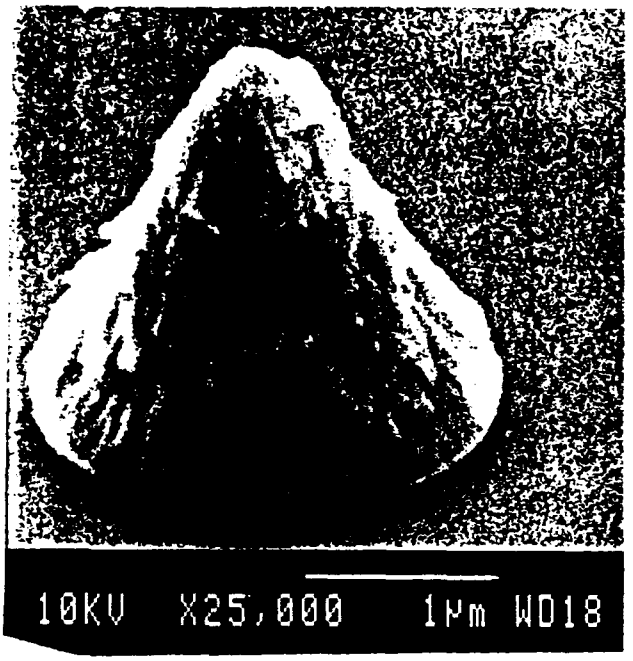

Figure 24 Scanning electron view of submicrometer tip formed by depositing titanium through a 3-μm self-closing hole.

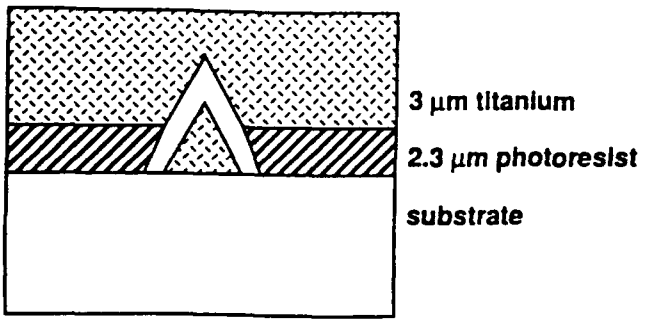

Figure 25 Process for forming the submicrometer tip.

To make submicron spatial resolution possible in testing integrated circuits, we have we have adapted the technology for forming rugged metallic cones from the field of vacuum microelectronics.[33, 34] This process employs conventional, repeatable photolithographic techniques to form tips with 100-nm-radius of curvature (figure **24**). This is done as follows: On a substrate suitable for photolithographic processing, a layer of photo-resist is hardened, patterned, and developed, leaving a 3-μm round hole at the location where a tip is desired. Deposition of a few microns of metal, such as titanium, simultaneously causes the growth of a conical tip at the base of this hole and the narrowing of its opening. This forms a sharp tip by virtue of the shrinking-aperture.

Subsequently, the thick metalization is removed by dissolving the photo-resist layer, as shown in figure **25**. The remaining structure is a sharp, rugged tip at a precisely defined location on the substrate. This recipe is compatible with a many other processes on GaAs and Si.

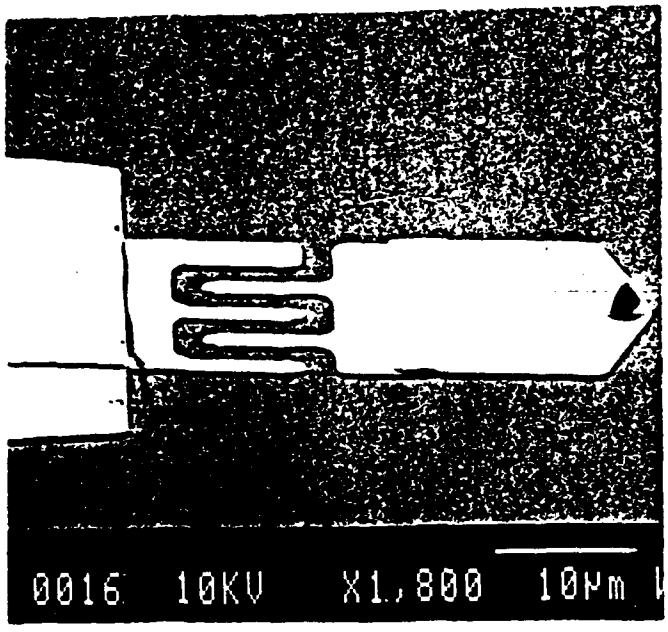

Figure 26 Scanning electron view of the integrated MSM gate and submicrometer tip on LT-GaAs.

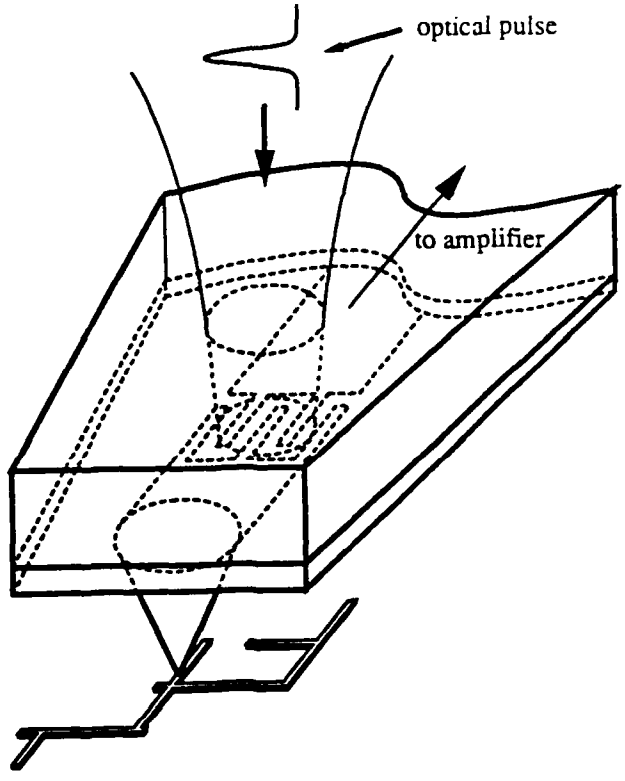

Figure 27 Position of nanoprobe relative to device under test.

Figure **26** shows a photomicrograph of the integrated photoconductive gate and the submicron tip. Figure **27** illustrates a typical experimental set-up for using the photoconductive probe. To facilitate optical access to the gate, we will eventually illuminate from the backside through the substrate. This would be accomplished by thinning the backside to a thickness of a few-micrometers. For this approach, a 2-μm-thick layer of $Al_{.70}Ga_{.30}As$ could be grown beneath the LT-GaAs layer as an etch stop. Light would then pass through the thin, transparent AlGaAs layer to excite the photoconductive gate. Alternatively, we could use topotaxial bonding to fix the semiconductor to a transparent substrate.

During the last 6 months, a high-speed, high-sensitivity probe was fabricated and tested in our laboratory. Using a crude 20-μm square tip with a 2-μm interdigital photoconductive sampling gate on LT-GaAs, the following results have been obtained: [34]

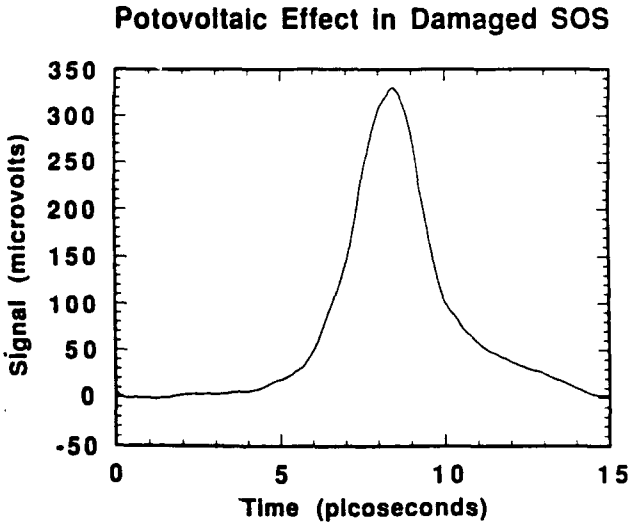

Figure 28 Measured waveform using a probe with a 20-μm tip.

- Sensitivity of ~1-μV/√Hz (the noise floor measured in figure **28**).
- Temporal resolution of 2 ps.
- Direct measurement of absolute voltages was demonstrated.
- Repeatable contact resistance was demonstrated.
- The 30-ps gate delay of a heterostructure insulated-gate FET enhancement/depletion mode inverter was measured.
- The probe was used in pulse mode to inject a picosecond signal onto a circuit. A second probe was used to time-resolve the picosecond response.

The variety of these results demonstrates the versatility of the photoconductive nanoprobe technology. The sensitivity of the external photoconductive sampling technique is also demonstrated by the clarity of the signal shown in figure **28**.

Summary of Results

The work carried out under this contract has yield steady progress *en route* to multi-hundred GHz optical communications. The conditions for velocity matching and high fidelity signal transmission in an optical modulator have been met. A wavelength-compatable high-speed photoconductive detector has been developed. Novel means of testing fast optical transients has been dedveloped. A probe which has the potential to test devices and circuits in the multi-hudred GHz range has been demonstrated. The key points of these results are outline below:

Modulator

- Propagation speed of electrical signals matches optical signal speed to within two parts in a thousand corresponding to <500-fs walk-off in 10mm.
- 1.4 ps pulse response is preserved over 10 mm of propagation at cryogenic temperatures
- 2.1 ps pulse response is preserved over 10 mm of propagation at room temperature.

Detector

- A wavelength-compatable MSM photoconductive detector based on LT-GaAs is demonstrated to have a 375 GHz bandwidth (-3-dB point), 0.1 A/W responsivity, and functionality for picosecond detection and gating.

High Voltage Switching

- 825 Volts is switched in LT-GaAs with a 1.4-ps rise time and a 4-ps width in a 100-μm-wide transmission line gap.

SOTA

- An optical sampling structure based on the LT-GaAs MSM photoconductive detector/gate is shown to have 1.9 ps resolution and pW sensitivity.

Picosecond Nanoprobe

- A novel external circuit probe based on the MSM technology is demonstated with 2.3 ps temporal resolution and absolute microvolt sensitivity.

References

1. J. F. Whitaker, J. A. Valdmanis, M. Y. Frankel, S. Gupta, J. M. Chwalek, and G. A. Mourou, Microelectron. Eng. 12, 369 (1990).
2. S. K. Korothy, G. Eisenstein, R. S. Tucker, J. J. Veselka, and G. Raybon, Appl. Phys. Lett., 50, 1631, (1987).
3. E. D. Palik, Handbook of Optical Constants and Solids, Academic Press Inc. 433, 1985.
4. J. Nees, S. Williamson, and G. Mourou, Appl. Phys. Lett., 54, 1962, (1989).
5. D. R. Grischkowsky, M. B. Ketchen, C-C. Chi, I. N. Duling III, N. J. Halas, J-M. Halbout, IEEE J. Quantum Electron. 24, 221 (1988).
6. J. Van Zeghbroek, W. Patrick, J-M. Halbout, and P. Vettiger, IEEE Electron Device Lett. 9, 527 (1988).
7. W. C. Koscielniak, J. L. Pelouard, and M. A. Littlejohn, Appl. Phys. Lett. 54, 567 (1989).
8. W. C. Koscielniak, J. L. Pelouard, and M. A. Littlejohn, IEEE Photon. Technol. Lett. 2, 125 (1990).
9. F. W. Smith, H. Q. Le, V. Diadiuk, M. A. Hollis, A. R. Calawa, S. Gupta, M. Frankel, D. R. Dykaar, G. A. Mourou, and T. Y. Hsiang, Appl. Phys. Lett. 54, 890 (1989).
10. T. Motet, J. Nees, S. Williamson, and G. Mourou, Appl. Phys. Lett. 59, 1455 (1991).
11. J. F. Whitaker, J. A. Valmanis, M. Y. Frankel, S. Gupta, J. M. Chwalek, and G. A. Mourou, Microelectron. Eng. 12, 369 (1990).
12. S. M. Sze, Physics of Semiconductor Devices, 2nd ed. (Wiley, New York, 1981), p. 746.
13. M. Y. Frankel, J. F. Whitaker, G. A. Mourou, F. W. Smith, A. R. Calawa, IEEE Trans. Electron Devices 37, 2493 (1990).
14. S. Gupta, J. Pamulatpati, J. Chwalek, P. K. Bhattacharya, and G. Mourou, in Ultrafast Phenomena VII, edited by C. B. Harris, E. P. Ippen, G. A. Mourou, and A. H. Zewail (Springer-Verlag, Berlin, 1990), p. 297.
15. J. B. D. Soole and H. Schumacher, IEEE Trans. Electron Devices 37, 2285 (1990).
16. S. Gupta, J. F. Whitaker, and G. A. Mourou, IEEE Microwave Guided Wave Lett. 1, 161, (1991).
17. C. Moglestue, J. Rosenzweig, J. Kuhl, M. Klingenstein, M. Lambsdorff, A. Axmann, Jo. Schneider, and A Hulsmann, J. Appl. Phys. 70, 2435 (1991).
18. D. L. Rogers,Picosecond Electronics and Optoelectronics II, edited by F. J. Leonberger, C. H. Lee, F. Capasso, and H. Morkoç (Springer-Verlag, Berlin, 1987).
19. S. M. Sze, Physics of Semiconductor Devices, 2nd ed. (Wiley, New York, 1981), p. 45.
20. D. G. Stearns, J. Appl. Phys., 65 (3), p. 1308 (1989).

21. T. Norris, T. Sizer II, and G. Mourou, "Generation of 85 fs Pulses by Synchronous Pumping of a Colliding Pulse Mode-locked Dye Laser", J. Opt. Soc. Am. B, **2**, April 1985.

22. I. N. Duling III, T. Norris, T. Sizer II, P. Bado, and G. Mourou, "Kilohertz Synchronouse Amplification of 85 fs Optical Pulses", J. Opt. Soc. Am. B, **2**, April 1985.

23. G. Iafrate, "High-Speed Transport in III-V Compounds", in Gallium Arsenide Technology, edited by D. K. Ferry, SAMS 1985.

24. M. C. Nuss and D. H. Auston, "Direct Subpicosecond Measurements of Carrier Mobility of Photoexcited Electrons in GaAs", in Picosecond Electronics and Optoelectronics II, edited by F. J. Leonberger, Springer-Verlag 1987.

25. D. H. Austin, Picosecond Optoelectronic Devices, edited by Chi H. Lee (Academic Press Inc., 1984), p. 73.

26. J. Van Zeghbroek, W. Patrick, J-M Halbout, and P. Vettiger, IEEE Transactions on Electron Devices, 37, 2493 (1990).

27. M. Klingenstein, J. Kuhl, J. Rosenzweig C. Moglestue, A. Axmann, Applied Physics letters, 70, 2435, (1991).

28. Martin van Exter, and Daniel Grischkowsky, IEEE Transactions on Microwave Theory and Techniques, MTT-38, 1684 (1990).

29. R. H. Kingston, Detection of Optical and Infrared Radiation (Springer-Verlag, Berlin, 1978), p. 58.

30. P. Ho, M.Y. Kao, P.C. Chao, K.H.G. Duh, J.M. Ballingall, S.T. Allen, A.J. Tessmer, P.M. Smith, Electron. Lett., 27, 325 (1991).

31. M.Y. Frankel, J.F. Whitaker, G.A. Mourou, and J.A. Valdmanis, "Ultrahigh-bandwidth vector network analyzer based on external electro-optic sampling," Solid-State Electronics, vol. 35, pp. 325-332 (Mar. 1992).

32. C.H. Lee, "Picosecond optics and microwave technology," IEEE Trans. on Microwave Theory Tech., vol. 38, May 1990, pp. 596-607.

33. C. Spindt, I. Brodie, L. Humphrey, and E. Westerberg, "Physical Properties of Thin Film Field Emission Cathodes with Molybdenum Cones," J. Appl. Phys., Vol. 37(12), December 1976.

34. J. Kim, S. Williamson, J. Nees, S. Wakana, "A Novel Free-Standing Absolute-Voltage Probe With 2.3-Picosecond Resolution and 1-Microvolt Sensitivity," Ultrafast Phenomena VII, 8-12 June, 1992, Antibes-Juan-Lesp-Pins, France.

Papers published or presented

- 1.4 Picosecond-Risetime High-Voltage Photoconductive Switching, T. Motet, J. Nees, S. Williamson, and G. Mourou, Applied Physics Letters, 59, 1984, 1991.
- 375-GHz-Bandwidth Photoconductive Detector, Y. Chen, S. Williamson, T. Brock, F. W. Smith, and A. R. Calawa, Applied Physics Letters, 59, 1455, 1991.
- S. Gupta, S. L. Williamson, Y. Chen, J. F. Whitaker, and F. W. Smith, Ultrafast Detectors using III-V Epilayers Grown by Molecular-Beam-Epitaxy at Low Temperatures, Laser Focus World, July 1992.
- 1.9 Picosecond Optical Temporal Analyzer using 1.2 Picosecond Photoconductor and Gate, Y. Chen, S. L. Williamson, T. Brock, F. W. Smith, IEEE International Electron Device Meeting, Washington D.C., 417, 1991.
- Development of a Multi-Hundred Gigahertz Electro-Optic Modulator and Photodetector, S. Williamson, Y. Chen, D. Craig, and G. Mourou, Proc. DOD Fiber Optics '92, 271 1992.
- Picosecond High-Voltage Pulses Generated Using Low-Temperature GaAs, T. Motet, J. Nees, S. Williamson, and G. Mourou, Conf. of Materials Research Society, Boston 1991.
- Multi-Hundred Gigahertz Photodector Development Using LT GaAs, Y. Chen, S. Williamson, T. Brock, F. W. Smith, and A. R. Calawa, Conf. of Materials Research Society, Boston, 1991.
- Efficient High Voltage Picosecond Photoconductive Switching, T. Motet, J. Nees, S. Williamson, and G. Mourou, at Picosecond Electronics and Optoelectronics IV in Salt Lake City, March '91
- Propagation of Picosecond Electrical Pulses in GaAs for Velocity-Matched Modulators, Y. Chen, J. Nees, and S. Williamson, at Picosecond Electronics and Optoelectronics IV in Salt Lake City, March '91.
- Single-Picosecond High-Voltage Photoconductive Switching Using Low-Temperature-Grown GaAs, T. Motet, J. Nees, S. Williamson, and G. Mourou, at Conference on Laser and Electro-Optics in Baltimore, May '91.
- 1.2 ps High-Sensitivity Photodetector/Switch Based on Low-Temperature-Grown GaAs, Y. Chen, S. Williamson, and T. Brock, at Conference on Lasers and Electro-Optics in Baltimore, May '91.

Patent Applications

- 1-Picosecond High-Sensitivity Photoconductor

Students Graduating

- Yi Chen, PhD in Electrical Engfineering, University of Michigan, May 1991